International Journal of Mass Spectrometry 277 (2008) 155–161

Contents lists available at ScienceDirect

International Journal of Mass Spectrometry

journal homepage: www.elsevier.com/locate/ijms

Following electron attachment to CS ($^1\Sigma$): Quantum scattering calculations of the lowest resonant state

F. Carelli[a,b], F. Sebastianelli[a,b], I. Baccarelli[c], F.A. Gianturco[a,b,*]

[a] Department of Chemistry, University of Rome 'La Sapienza', P.le Aldo Moro 5, 00185 Roma, Italy
[b] INFM, Italy
[c] CASPUR Supercomputing Consortium, via dei Tizii 6, 00185 Rome, Italy

ARTICLE INFO

Article history:
Received 17 March 2008
Received in revised form 18 July 2008
Accepted 18 July 2008
Available online 30 July 2008

This work is affectionately dedicated to Professor Eugen Illenberger, a very good scientist and a dear friend, on the occasion of his 65th birthday.

Keywords:
Carbon monosulphide
Electron-molecule collisions
Resonant states
Scattering calculations

ABSTRACT

Parameter-free scattering calculations are carried out for the CS ($^1\Sigma^+$) molecular target interacting with slow electrons (<10 eV) using a quantum dynamical approach in the molecular reference frame and varying the internuclear distance over a sizeable range of values. The calculations find a resonant state of $CS^-(^2\Pi)$ in the low-energy region and the resonance is seen to stabilize as a bound CS^- molecule when the bond is stretched beyond the CS equilibrium value, in agreement with existing experiments and calculations. An analysis of the excess, metastable electron is able to show that the initially occupied d π^*-orbital of the molecular resonance evolves into a more localized p*-orbital on the sulphur fragment. The results from the calculations are related to the existing experimental data for the title system and to the information we have on the target molecule electron affinity.

1. Introduction

Carbon monosulphide is known to be formed in cold plasmas of sulphur and carbon and is considered to be of major importance because of its expected etching properties [1,2]. One knows, in fact, that plasmas with sulphur precursors can be used in chemical vapour depositions (CVD) to place S in the structure of diamond films after discharge-induced break-up of CS and CS_2 produced by the reaction in the CVD environments [3]. The CS molecule may also play a role in atmospheric reactions, where it can activate the production of OCS, considered to be a possible source for the formation of S-containing aerosols in the Earth's atmosphere [4]. Because of its abundance in space, CS has been observed in molecular clouds [5], in circumstellar envelopes [6], in comets [7], and in other galaxies [8]. It is a molecule often described as a radical, although in its ground state the outer electronic configuration is given by: $\ldots 7\sigma^2 2\pi^4(^1\Sigma^+)$. Recent experimental studies [9] have focused on the dissociative electron attachment (DEA) to CS from electron scattering experiments and have considered the following reactions

$$\begin{aligned} CS(^1\Sigma^+) + e^- \rightarrow (CS^-)^* &\rightarrow S^-(^2P) + C(^3P) \\ &\rightarrow S^-(^2P) + C(^1D) \\ &\rightarrow C^-(^4S) + S(^3P). \end{aligned} \quad (1)$$

as important processes where the formation of intermediate resonant states was postulated to occur before the ensuing bond break-up induced by the above reactions. Since the appearance potentials for the three channels were at 5.43 eV, 6.70 eV and 6.40 eV, respectively, the authors [9] suggested that different resonant states were formed from an initial, low-energy shape resonance into a π^* orbital which is combined with core excitation processes of valence electrons during the primary attachment (i.e., the occurrence of a variety of Fesbach-type, core-excited resonances). The presence of low-energy shape resonances (<3.0 eV) has, in fact, been detected in similar molecules like CO, N_2O, CS_2 and OCS, where such resonances into $^2\Pi$ states have been observed [10–12] and also computed [13–15] at energies below 2.0 eV. On the other hand, so far no direct measurements nor computational scattering studies have found its existence for the CS molecular target. Earlier experimental work [16] has reported measurements of its electron impact total ionization cross-sections, which were in turn

* Corresponding author at: Department of Chemistry, University of Rome "La Sapienza", P.le Aldo Moro 5, 00185 Roma, Italy. Fax: +39 06 49913305.
E-mail address: fa.gianturco@caspur.it (F.A. Gianturco).

1387-3806/$ – see front matter © 2008 Elsevier B.V. All rights reserved.
doi:10.1016/j.ijms.2008.07.015

theoretically computed using the binary-encounter-Bethe model [17]. More recent calculation [18], have examined the behaviour of the angular distributions in the low and intermediate energy range by employing a complex, model optical potential that included static, exchange and model correlation-polarization effects but could not be compared with any differential cross-section measurements. However, in the low-energy range (<10 eV) their limited inclusion of correlation effects and examined range of energies showed the presence of broad $^2\Pi$ and $^2\Delta$ shape resonances below 7 eV, in contrast with what they found for N_2O, where a clear $^2\Pi$ resonance appeared around 2 eV of collision energy: the latter resonance has also been observed in our earlier calculations on N_2O [19]. Furthermore, their calculations did not go below 1 eV of energy but found the $^2\Pi$ partial cross-section energy dependence at threshold to very likely have to go through some maximum value before zero energy. In conclusion, the possible presence of a primary, low-energy shape resonance in the CS polar system (dipole moment, $\mu = 0.773$a.u. [20]) postulated in earlier studies, so far has not been confirmed either by calculations or by direct measurements of elastic cross-sections in that energy range. We have therefore decided to undertake such a study in order to look for both the presence of a low-energy single-channel resonance and for its possible role in describing the nuclear stretching behavior of the temporary anionic species. We shall show below that our calculations have indeed found a low-energy $^2\Pi$ resonant state, and that we are able to describe the spatial shape of the excess electron in this transient species. The following Section 2 reports an outline of our quantum treatment of the scattering process, while Section 3 gives an analysis of our computational results. The present conclusions are gathered in Section 4.

2. The computational modelling

2.1. Scattering equations in a single center expansion

In the Born-Oppenheimer (BO) approximation one represents the total wave function of the "target + e^-" as an antisymmetrized product of electronic wave functions which parametrically depend on the positions of the nuclei. The scattering process under investigation is here initially limited to elastic channels, therefore no excitations are considered, and the N bound electrons of the target are assumed to be in a specific molecular electronic state (ground state) which is taken to remain unchanged during the scattering. The target electronic wave function is given by the self-consistent-field (SCF) approximation with a single determinant description of the N occupied molecular orbitals (MOs). In our scattering equations the occupied MOs of the target are expanded on a set of symmetry-adapted angular functions with their corrisponding radial coefficients represented on a numerical grid [21]. In this approach, any arbitrary three-dimensional function describing a given electron, either a bound or a scattering electron, is expanded around the center of mass of the molecule, where the origin of the body-fixed frame is placed. The single center expansion (SCE) is then

$$F^{p\mu}(r, \hat{\mathbf{r}}|\mathbf{R}) = \sum_{l,h} r^{-1} f_{lh}^{p\mu}(r|\mathbf{R}) X_{lh}^{p\mu}(\hat{\mathbf{r}}), \tag{2}$$

where the indices refer to the μ th component of the p th irreducible representation (IR) of the point group of the molecule at the nuclear geometry $\mathbf{R}$. The angular functions $X_{lh}^{p\mu}(\hat{\mathbf{r}})$ are symmetry-adapted angular functions given by the proper combination of harmonics $Y_{lm}(\hat{\mathbf{r}})$

$$X_{lh}^{p\mu}(\hat{\mathbf{r}}) = \sum_m b_{lmh}^{p\mu} Y_{lm}(\hat{\mathbf{r}}). \tag{3}$$

The coefficients $b_{lmh}^{p\mu}$ are discussed in the literature and can be obtained from a knowledge of the character tables of the relevant molecular point group [22]. The coupled, partial integro-differential scattering equations take the form

$$\left[\frac{d^2}{dr^2} - \frac{l(l+1)}{r^2} + 2(E - \epsilon_\alpha)\right] f_{lh}^{p\mu\alpha}(r|\mathbf{R}) = 2 \sum_{l'h'p'\mu'\alpha'} \int dr' V_{lh,l'h'}^{p\mu\alpha,p'\mu'\alpha'}(r, r'|\mathbf{R}) f_{l'h'}^{p'\mu'\alpha'}(r'|\mathbf{R}), \tag{4}$$

where E is the collision energy and ϵ_α is the electronic eigenvalue for the α th asymptotic state so that $k_\alpha^2/2 = E - E_\alpha$ where k_α is asymptotic momentum of the electron with the target in a state α. The (p, μ, α) indices in Eq. (4) now label the symmetry and corresponding target state of the continuum wave function, and refer to the kernel of the integral operator $\hat{V}$, a sum of diagonal and nondiagonal terms that in principle fully describe the electron-molecule interaction during the collision. The choice of a single state α obtains the exact-static-exchange (ESE) representation of the electron-molecule interaction for the molecular ground state geometry $\mathbf{R}$. Introducing the further assumption of having only a local e^--molecule interaction (as we shall also discuss below) one can again simplify the form of the coupled equations

$$\left[\frac{d^2}{dr^2} - \frac{l_i(l_i+1)}{r^2} + k^2\right] f_i^{p\mu}(r|\mathbf{R}) = \sum_j V_{ij}^{p\mu}(r|\mathbf{R}) f_j^{p\mu}(r|\mathbf{R}), \tag{5}$$

where the indexes i or j represent the "angular channel" (l, h) and the potential coupling elements are given by

$$V_{ij}^{p\mu}(r|\mathbf{R}) = \langle X_i^{p\mu}(\hat{\mathbf{r}})|V(\mathbf{r}|\mathbf{R})|X_j^{p\mu}(\hat{\mathbf{r}})\rangle = \int d\hat{\mathbf{r}} X_i^{p\mu}(\hat{\mathbf{r}}) V(\mathbf{r}|\mathbf{R}) X_j^{p\mu}(\hat{\mathbf{r}}). \tag{6}$$

In this study we model the exchange contribution to the operator of Eq. (5) with an energy-dependent local exchange potential suggested by Hara [23], as discussed many times before [24]. We further include the dynamical short-range correlation through the addition of a local energy-independent potential which is obtained by defining an average dynamical correlation energy of a single electron within the formalism of the Kohn and Sham variational scheme. The functional derivative of such a quantity with respect to the SCF N-electron density of the molecular target provides a density functional description of the required short-range correlation term that is an analytic function of the target electron density [21,24]. The latter contribution is finally connected with the long-range dipole polarizability term providing the additional polarization potential contribution, as given in detail by [21]. The above modelling of the full interaction for an electron impinging on an many-electron target has been used by us many times before, finding rather good agreement with the available experimental data [14,15,19,21,24].

2.2. The adiabatic potential model

The main focus of this paper is to examine the mechanism and qualitative characteristics of a possible low-energy, one-electron resonance and its evolution along the lower part of the molecular potential energy curve (PEC) of the temporary anion. This requires a model which is simple enough to be computationally attractive

but which includes sufficient details of the full scattering problem to reproduce the essential features of the physics involved. Thus, we look at the low-energy resonances also by using a simple, purely local model potential that we have called the static model-exchange correlation (SMEC) potential, V_{SMEC} [21]. We start by noting that the standard, symmetry adapted angular momentum eigenstates, $X_{lh}^{p\mu}$, do not form the most compact angular set for the e$^-$-molecule scattering problem: an alternative basis expansion is provided, instead, by the angular eigenfunctions obtained by diagonalizing the angular Hamiltonian at each radius r. These distance-dependent angular eigenstates are referred to as the adiabatic angular functions (AAFs) $Z_k^{p\mu}(\theta, \phi, r)$which, at each radial value, are linear combinations of the symmetry-adapted "asymptotic" harmonics discussed before

$$Z_k^{p\mu}(\theta, \phi, r) = \sum_{lh} X_{lh}^{p\mu}(\theta, \phi) C_{lh,k}(r), \tag{7}$$

where the expansion coefficients are solutions of the matrix eigenvalue equation

$$\sum_{lh} V_{l'h',lh}(r) C_{lh,k}(r) = C_{l'h',k}(r) V_k^A(r). \tag{8}$$

The eigenstates $V_k^A(r)$ now form an adiabatic radial potential for each index k over the selected range of the e$^-$-molecule distances. The spatial extent of the resonant wave function can be determined from the well and angular momentum barrier of such adiabatic potential terms and the physical mechanism for the resonance is that of a trapped electron tunneling through the potential barrier. In order to avoid the nonadiabatic coupling terms between adiabatic curves, we actually employ a piecewise diabatic (PD) representation of the potential whereby the radial coordinate is divided into a number of regions so that sector i is defined as $r_{i-1} < r < r_i$, with $r_0 = 0$. In each radial region we average the coupling potential $V_{l'h',lh}(r)$ over r and the resulting averaged potential is diagonalized as in Eq. (8) to yield a set of angular functions $Z_{k,i}^{p\mu}(\theta, \phi)$. Then, in region i the scattering potential is transformed into the new representation in which it is nearly diagonal. The resulting equations are solved using the full scattering potential in each region with the further approximation of ignoring the off-diagonal couplings in that region: to solve the radial equations using the PD approach requires matching of the radial functions and their derivatives at the boundary between radial regions. The transformation of the radial functions from one region to the next is given by the transformation matrix $U_{k,k'}^{(i+1\leftarrow i)}$ defined by

$$U_{k,k'}^{(i+1\leftarrow i)} = \sum_{lh} C_{lh,k}^{(i+1)} C_{lh,k'}^{(i)}. \tag{9}$$

When the size of the angular momentum eigenfunction basis used is larger than the size of the diabatic angular basis set, the transformation matrix $U_{k,k'}$ is not in general unitary. We accomplish the unitarization of $U_{k,k'}^{(i+1\leftarrow i)}$ using simple Graham-Schmidt orthonormalization on the columns of $U_{k,k'}^{(i+1\leftarrow i)}$. The above treatment, being easier in terms of computational cost, usually finds the resonances slightly shifted from those given by the full coupled-channel solutions of Eq. (5)[21]. However, their nature and general features remain unchanged and of the same physical significance, while allowing for a reduction of the computational effort.

3. Results and discussion

3.1. Locating the $^2\Pi$ resonance

The target MOs were obtained using a conventional representation over a Gaussian basis set and the quality of the expansion

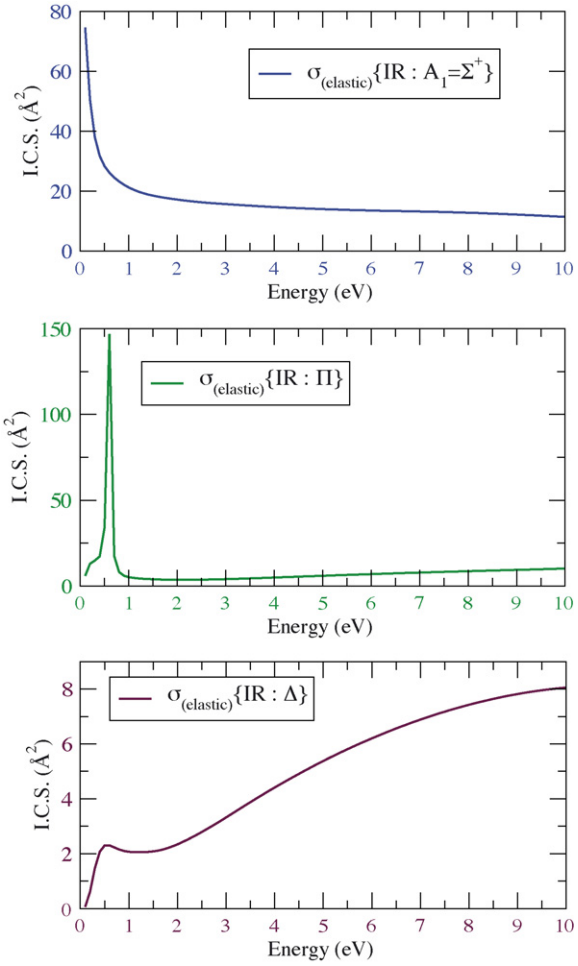

Fig. 1. Computed partial, elastic integral cross-sections (I.C.S.) for the three dominant contributions to e$^-$-CS($^1\Sigma$) scattering from thresold to 10 eV. See text for details.

was given by a D95* expansion [25]. The bond length initially employed for the equilibrium geometry was 1.53 Å [16]. The size of the physical "box" that contains the diabatized potential terms described before was 15 Å and the overall radial and angular grids (r, ϑ, φ) included 1300 × 84 × 324points. The single-center-expansion for the potential was checked for convergence on the final cross-sections and included terms up to $\lambda_{max} = 50$. Likewise, the corresponding partial wave expansion for the scattered electron was carried out up to $l_{max} = 100$. The calculated wave function for the neutral target yielded a permanent dipole moment value of $\mu_{eq} = 0.60$a.u., not far from experiments [20], as mentioned before. Since we are chiefly interested in locating the possible existence of a low-energy resonance, an essentially short-range effect of dynamical trapping of the scattered electron, we did not include the dipole correction [27] when generating the elastic integral cross-sections (rotationally summed) of the present study. In any event, the following discussion will only focus on the resonance properties and behaviour as a function of bond deformations, hence will be largely independent of long-range effects [28]. The actual energy behaviour of the dominant symmetry components which make up the electron scattering elastic cross-sections from the CS fragment is depicted, up to 10 eV, in the three panels of Fig. 1. We report there the partial elastic cross-sections for the $^2\Sigma$ (top panel), $^2\Pi$, (middle panel) and $^2\Delta$ (bottom panel). Since the dipole correction in the molecular frame is not included, we do not expect that the size

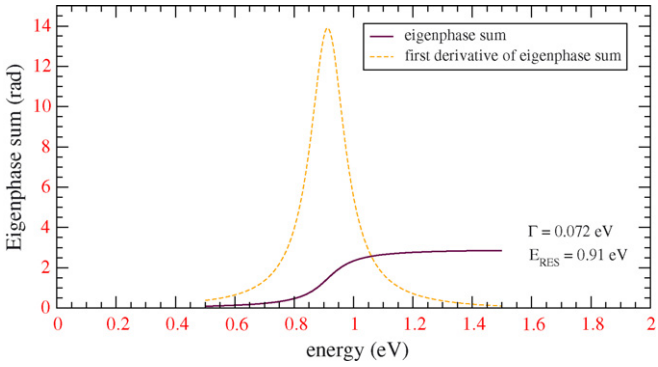

Fig. 2. Computed eigenphase sum within the $^2\Pi$ scattering component and behaviour of the delay matrix from its derivative. See Ref. [28] for details.

of the three components of our total, elastic cross-sections are converged in the low energy region. However, we are here interested in revealing the possible presence of a shape resonance, i.e., of a short-range effect largely independent of such a correction [26]. All the calculations of Fig. 1 were done at the R_{eq} value of the neutral target molecule.

The results clearly show the presence of one low-energy (∼0.6 eV) shape resonance appearing as a strong peak in the $^2\Pi$ component. One should note that such a low energy occurrence was also surmised by experimentalists as a precursor for higher-energy resonances [9], while the broader feature of the $^2\Delta$ contribution, shown by the present study, was also suggested by earlier calculations on this molecule [18], which however did not go down enough in energy to reach the low-energy resonance position we find here in the $^2\Pi$channel. Their Fig. 7, however, indicates that their corresponding partial cross-section below 1.0 eV should go through a maximum before vanishing at zero energy. The dipole-induced threshold behaviour is also visible in the totally-symmetric contribution, the $^2\Sigma$ state, which however does not show any resonance. To better analyse the scattering features, we report in Fig. 2 the behaviour of the eigenphase sums for the $^2\Pi$ symmetry, together with their first derivative: it allows us to extract the pure resonant component from the background and to obtain the resonance width from the lorentzian fit of the delay matrix (see for details Ref. [28]). Thus, we clearly see that the CS molecule, at its equilibrium geometry, shows the presence of a resonant state close to threshold.

These calculations were done using the adiabatic potential model, hence it is not surprising that the resonance position is slightly shifted by about 0.2 eV with respect to the full calculations of Fig. 1. No marked modifications of the physical behavior have however been detected. The calculations now show the shape resonance around 0.9 eV, with a width of 72 meV, corresponding to a lifetime of a few ps. Furthermore, if we wish to extract the dominant partial wave that contributes to the dynamical trapping of the resonant electron, we need to examine the behaviour of the dominant components of the diabatic potential: our calculations included up to 50 terms of that potential in order to reach convergence for the results of Fig. 1, while only the lower ten were found important for the resonant trapping mechanism analysed via the adiabatic potential. The energy dependence of the lower components is given by Fig. 3, where angular momenta up to $l = 5$ are shown.

One can clearly see, at least qualitatively, that the scattering region around 1 eV, where the resonance is found to occur, shows two dominant potential curves for $l = 1$ and 2, with the latter angular momentum producing the dynamical trapping. Thus, one can suggest that the $^2\Pi$ resonance corresponds to what is conventionally called an electron capture into an antibonding π^* orbital of the neutral parent molecule: $[\ldots 7\sigma^2 2\pi^4] \rightarrow [\ldots 7\sigma^2 2\pi^4 3\pi^1]$. However, the scattering calculations do point at a slightly more complicated picture, where the scattering electron should be described by the several angular momenta which contribute to the scattering process, although the dominant effects come from an $l = 2$ trapping (i.e., a resonant πd-type orbital) and from non-adiabatic coupling with a decay channel of $l = 1$ (i.e., of πp-symmetry). It is also interesting to note that earlier, high quality, quantum chemical calculations [30] described the potential energy curves of $CS^-(^2\Pi)$ and $CS(^1\Sigma)$ and found that the anionic species, at the R_{eq} value of the neutral is *not* stable with respect to electron detachment. As they stretched the C — S bond, however, they detected a positive, but essentially negligible value (0.020 eV) for the system electron affinity (EA), so that it was necessary to shift the anionic curve down with respect to the neutral PEC to reach the experimental EA value of ∼0.20 eV. These results therefore suggest the presence of a very weakly bound anionic species, obtained via variational calculations with a discrete basis set with bound-state boundary conditions for a stretched target but not for the initial geometry. No scattering calculations were performed there and therefore no resonant states at R_{eq} could have possibly been detected. As mentioned above, the present study finds a threshold resonant state of the same symmetry but also no bound state around the equilibrium geometry. Since the possible existence of a slightly stable, bound anionic species as the bond is stretched is what Ref. [30] indicates, it becomes interesting to see what happens to our resonant state as the bond is stretched. This feature will be discussed in the following section. Finally, it should also be noted the earlier experiments [29] detected a stable CS^- species *only* for a stretched geometry with respect to the CS parent molecule, in keeping with our finding (see below) and with those of [30].

3.2. Bond deformation effects

In order to further analyze the possible evolution of the present resonance, we repeated our adiabatic potential calculations for different nuclear geometries, moving from a rather "compressed" molecule with $R_{CS} = 1.1$ Å to a more stretched molecule with $R_{CS} = 1.64$ Å, beyond which no pole in the S-matrix was found for locating a resonance in that energy region: i.e., the stretched molecule potential causes the *S*-matrix pole to move to the negative energy axis of the complex plane, thereby forming an anionic bound state;

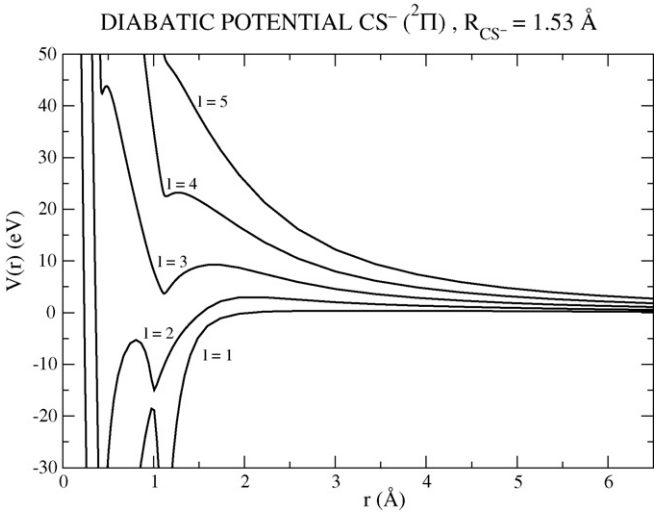

Fig. 3. Computed Diabatic potential terms employed for the calculation of the partial cross-section of $^2\Pi$ symmetry.

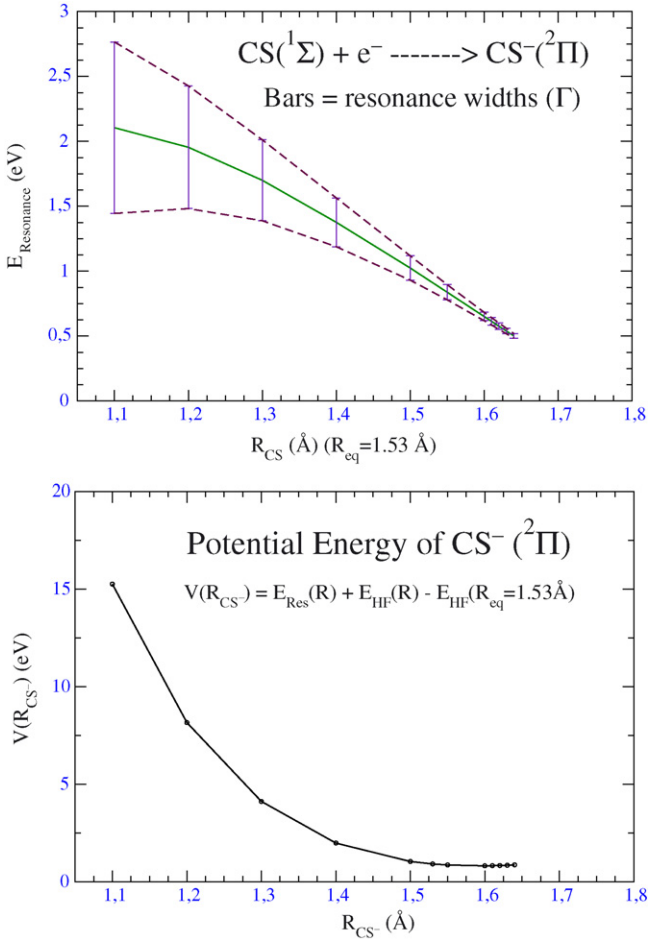

Fig. 4. Upper panel: computed changes of the $^2\Pi$ resonant features (E_{res} and Γ_{res} as a function of the molecular bond values. The equilibrium bond distance is 1.53 Å. Lower panel: potential behaviour (real part) of the $(N+1)$ electron system. See text for details.

it also causes the resonance not only to change its energy location but also to vary its lifetime, i.e., its width. We therefore describe both changes by representing location and width dependance versus bond distances on the same plot, as reported in the upper panel of Fig. 4.

The data in the panel clearly show the physical evolution of the resonant state as the molecular bond is deformed: when we compress the bond and move to a more "united atom" situation (Ti), the overall interaction with the impinging electron becomes more repulsive and the resonant state goes up in energy and becomes more unstable, i.e., it acquires a broader width and a shorter lifetime, becoming more likely to decay via electron detachment. On the other hand, when the bond gets stretched beyond its equilibrium value, the resonance moves down, closer to the zero-energy threshold, and becomes increasingly more stable, i.e., with longer lifetimes. The present calculations further find that when the bond is in the range of 1.61–1.64 Å the resonance has moved to much lower energies and acquired very narrow widths of a few meV: i.e., is becoming a stable $CS^-(^2\Pi)$ anionic species and the S-matrix pole has disappeared.

The lower panel of Fig. 4 shows the overall behaviour of the $(N+1)$ electron system when we add to the resonance energy the electronic energies of the target N-electrons and use the $CS(R_{eq})$ energy value as a reference (i.e., as zero of our local scale). The circles show our computations with the data of the upper panel, our computed Hartree–Fock energies of the N-electron target states at the various geometries and their scaling to the N-electron energy at R_{eq}. We see that the metastable "anionic" potential produced by our scattering calculations describes a system where the nuclei are bound and now exhibit a shifted minimum geometry between 1.60 and 1.61 Å. Furthermore, the extra electron is increasingly bound to the molecule for longer times, resembling as much as possible a bound electron within the anionic complex. The corresponding zero-point-energy (ZPE) of the bound nuclei in the metastable potential was found here to be 560 cm^{-1} [31]: it is interesting to note that the corresponding ZPE values for the very weakly bound anionic species $CS^-(^2\Pi)$ discussed by experiments [29], and by calculations [30], were found to be similar: around 600 cm^{-1} and about 500 cm^{-1}, indicating a similar shape of their nuclear PECs.

The evolution of the resonance could be additionally followed by looking at the changes in the spatial shape of the resonant wavefunction, depicted by us as intensity isolines over the molecular space containing the nuclear configurations [21]. The results for the present system are shown by the three panels of Fig. 5, where three different bond distances are considered. When we look at the compressed bond situation of the left panel, we see that the nearly-free scattered electron now acquires the shape of a molecular d_{xz} orbital along the z-axis which contains the molecule: the broader resonance moves towards the united-atom picture, something resembling a (Ti^-) broad resonance into one of the $3d^*$ orbitals of that atom. On the other hand, the resonant orbital at the equilibrium geometry (central panel) resembles instead a molecular (fully delocalized) πd orbital which has a clear antibonding plane across the C—S bond and slightly higher density over the S atom. Thus, our qualitative analysis of the resonant electron suggests it to be similar

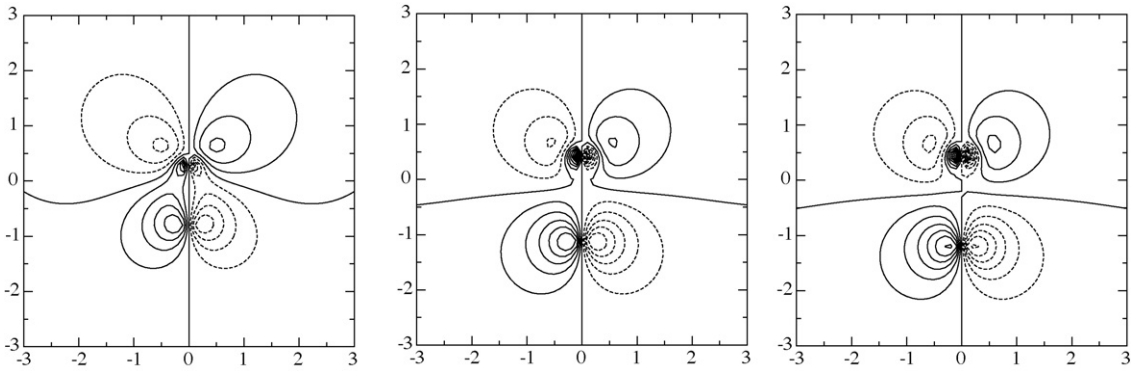

Fig. 5. Resonant wavefunction maps over the molecular xz-plane for three different bond distances. The S atom is above and the C atom is below, along the z-axis. Left panel: $R_{CS^-} = 1.10$ Å; centre panel: $R_{CS^-} = 1.53$ Å; right panel: $R_{CS^-} = 1.64$ Å.

to a d-type orbital of the united-atom when the bond is compressed, to look like a molecular π^*-orbital with d character at the equilibrium geometry and to finally evolve, as the bond is stretched, into a S-centered p*-type orbital which will stabilize asymptotically into an anionic bound state of the sulphur atom. However, within the region of bond distances sampled by our scattering calculations we already observe that the $(N+1)$ electron complex corresponds to a bound CS plus the extra electron stabilized into a very-long lived resonant state which is describing an anionic $CS^-(^2\Pi)$ molecule.

Computational work on the photoelectron spectroscopy of CS^- [30] that used accurate quantum chemical calculations had found, as discussed before, the existence of an anionic state where the extra electron is added to a molecular 3 π orbital to form a $^2\Pi$ configuration which is however not energetically stable with respect to the neutral parent molecule at its equilibrium geometry, while becoming only slightly so (by about 20 meV) when the molecular bond is stretched to larger values (1.635 Å). The present scattering calculations suggest that the title system is capable of supporting a threshold shape resonance at equilibrium geometry due to angular momentum dynamical trapping and that such a state can then also evolve into a stable CS^- bound state upon bond stretching up to ~1.64 Å. Earlier experiments [29] also provided indirect evidence for a clear bond lengthening (up to about 1.63 Å) upon stabilization of the anionic species, i.e., a value close to our estimate. In order to follow more in detail the above process by taking advantage of the resonance features uncovered by our present calculations, it would be of interest to look at the full shapes of the potential energy curves for the metastable $CS^-(^2\Pi)$ and the stable $CS(^1\Sigma)$ molecules which describe their electronic bound states. One could then compare the lower-lying $^1\Sigma$ state PEC [32,33] with that suggested by our present scattering calculations, which surmise the existence of a metastable $^2\Pi$ state that lies above the parent molecule at R_{eq}, by looking at our PEC for the metastable state (real part) reported by Fig. 4 in relation to that for the neutral molecule ($^1\Sigma$) obtained from accurate spectroscopic information [32,33]. Further more detailed scattering calculations and more extended ab initio computations for such curves are currently under way in our laboratory and will be reported elsewhere.

4. Present conclusions

This work has carried out a computational study on the possible existence of an intermediate $^2\Pi$ resonant state of the anionic CS molecule at low energies. The presence of an initially metastable state leading to the formation of higher, Fershbach-type resonances above 5 eV had been postulated before [9], but no explicit scattering calculations had been carried out to uncover its general features. The present study has focused on the modelling of the lower, metastable $^2\Pi$ state from quantum scattering calculations using a time-independent, coupled-channel approach employed by us before for several other molecular gases. The corresponding interaction potential has been assembled by including the exact static component, a DFT treatment of correlation-polarization effects and a DFT-based, model exchange potential (see previous Section 2). The method and model have been used by us on several polyatomic gases, and on $H_2$and N_2[34,35], with excellent agreement with experiments, over many years. The results of the scattering calculations with a CS target at its equilibrium geometry have shown the clear presence of a π^* resonance (with lifetime of the order of *fs*) with dominant $l=1$ and 2 partial wave components. The corresponding resonant excess electron has been shown to have the spatial shape of a d π^* orbital localized over the two atomic nuclei. Upon stretching the CS bond our calculations found that the resonant state keeps its π^* character, albeit shifting towards the *S* side as the two atoms separate. In the latter case, we found that between 1.61 and 1.64 Å the resonance becomes narrower and then disappears into a bound state of the $CS^-(^2\Pi)$ as the bond is stretched. This value is not far from the experimental estimates [29] for the stable bound state and from the quantum calculations of a very weakly bound anion [30] which indicate ~ 1.63 Å. The actual location of the resonance at R_{eq} of the neutral could, of course, change as more accurate models of the interaction are employed: in any event, however, we have shown that a detailed analysis of the scattering attributes of the $CS(^1\Sigma)$ molecular gas allows us to obtain specific information on the evolution of a shape resonance that describes the low-energy intermediate $^2\Pi$ state, a state found to be important in the study of several dissociative electron attachment decay channels observed [9] at higher energy for the parent molecule. In conclusion, the present quantum dynamical calculations have shown the following:

(i) that the $CS(^1\Sigma)$ molecule, at its equilibrium geometry, can attach an extra electron into a resonant state of $^2\Pi$ symmetry and that the state is a narrow resonance located around 600–900 meV above threshold;
(ii) that upon stretching of the bond up to 1.61–1.64 Å the resonance signature disappears into a bound state of the anionic species.

The earlier experiments [29] had also found that a stable beam of CS^- molecules corresponded to a stretched bond value of 1.627 Å. Furthermore, accurate quantum-chemistry calculations [30] found a very weakly bound CS^- species of $(^2\Pi)$ symmetry that also corresponded to a stretched bond (1.635 Å). Finally, earlier scattering calculations [18] did not go down enough on the energy scale to see the $^2\Pi$ resonance at R_{eq} but showed a rising feature in that partial cross-section below 1 eV, in keeping with our results. The present calculations have thus established the presence of an intermediate resonant state near threshold for the equilibrium geometry of $CS(^1\Sigma)$, a result which is not contradicted by existing experiments and calculations and which provides useful information on the possible structures of the intermediate species of reactions (1).

Acknowledgments

The financial support of the University of Rome Research Committee, of the Ministery of University National Research Project PRiN 06 and the CASPUR Supercomputing Consortium is gratefully thanked.

References

[1] L.G. Christophorou, D.L. Mc Carkle, A.A. Christodoulides, L.G. Christophorou, in: Electron-Molecule Interactions and Their Applications, Academic, New York, 1984.
[2] E.K. Moltzen, K.J. Klabunde, A. Senning, Chem. Rev. 88 (1988) 391.
[3] J.R. Petherbridge, P.W. May, G.M. Fuge, K.N. Rosser, M.N. Ashfold, Diamond Related Mater 11 (2002) 301.
[4] P.J. Crutzen, Geophys. Res. Lett. 8 (1981) 765.
[5] J.P. Williams, L. Blitz, Astrophys. J. 494 (1998) 657.
[6] P.M. Woods, F.L. Schoier, L.A. Nyman, H. Olofsson, Astron. Astrophys. 402 (2003) 617.
[7] N. Biver, et al., Earth Moon Planets 78 (1997) 5.
[8] S. Martin, J. Martin-Pintado, R. Manersberger, C. Henkel, S. Garcia-Burillo, Astrophys. J. 620 (2005) 210.
[9] K. Graupner, T.A. Field, L. Feketova, New J. Phys. 8 (2006) 314.
[10] R. Dressler, M. Allan, M. Tronc, J. Phys. B: At. Mol. Phys. 20 (1987) 393.
[11] C. Szmytkowski, M. Zubek, Chem. Phys. Lett. 57 (1978) 105.
[12] S.J. Buckman, B. Lohmann, Phys. Rev. A 34 (1986) 1561.
[13] F.A. Gianturco, P.G. Burke, N. Chandra, Mol. Phys. 27 (1974) 1121.
[14] T. Stoecklin, F.A. Gianturco, Eur. Phys. J. D 42 (2007) 85.
[15] T. Stoecklin, F.A. Gianturco, Chem. Phys. 332 (2007) 145.
[16] R.S. Freund, R.C. Wetzel, R.J. Shul, Phys. Rev. A 41 (1990) 5861.
[17] Y.-K. Kim, N.M. Weinberger, M.A. Ali, M.E. Rudd, J. Chem. Phys. 106 (1997) 1026.
[18] A.M.C. Sobrinho, M.-T. Lee, Int. J. Quant. Chem. 103 (2005) 703.

[19] T. Stoecklin, F.A. Gianturco, Eur. Phys. J. D 40 (2006) 369.
[20] G. Winnewisser, R.L. Cook, J. Mol. Spectrosc. 28 (1968) 266.
[21] R.R. Lucchese, F.A. Gianturco, Int. Rev. Phys. Chem. 15 (1996) 429.
[22] S.L. Altman, P. Herzig, Point-group Theory Tables, Oxford University Press, Oxford, 1994.
[23] S.J. Hara, J. Phys. Soc. Jpn. 22 (1967) 710.
[24] R. Curik, F.A. Gianturco, R.R. Lucchese, N. Sanna, J. Phys. B 34 (2000) 59.
[25] M.J. Frisch et al., Gaussian 03, revison c.02 (2004) Gaussian Inc., Wallingford, CT, 2004.
[26] F.A. Gianturco, P. Paioletti, K.H. Becker, Novel Aspects of Electron-Molecule Scattering, World Scientific Publ., 1998, p. 256.
[27] Y. Itikawa, Theor. Chem. Acc. 105 (2000) 123.
[28] F.T. Smith, Phys. Rev. 118 (1960) 349.
[29] S.M. Burnett, C.S. Felgerle, A.E. Stevens, W.C. Lineberger, J. Phys. Chem. 86 (1982) 4486.
[30] M. Hochlaf, G. Chamboud, P. Rosmus, T. Andersen, H.J. Werner, J. Chem. Phys. 11835 (1999) 110.
[31] R.J. LeRoy, Level Programme, U.W. Chem. Phys. Res. Rep. (November 2007).
[32] P. Coppens, J.C. Reynard, J. Drowart, J. Chem. Soc. Faraday Trans. II 75 (1979) 292.
[33] K.P. Huber, G. Herzberg, Molecular Spectra and Molecular StructuresIV Constants of Diatomic Molecules, Van Nostrand-Reinhold, New York, 1979.
[34] S. Telega, F.A. Gianturco, Eur. Phys. J. D 36 (2005) 271.
[35] S. Telega, F.A. Gianturco, Eur. Phys. J. D 38 (2006) 495.